A statistical investigation of dayside magnetosphere erosion showing saturation of response

Stefan Mühlbachler,[1] Charles J. Farrugia,[2] Joachim Raeder,[2] Helfried K. Biernat,[3] and Roy B. Torbert[2]

Received 8 April 2005; revised 9 August 2005; accepted 20 August 2005; published 11 November 2005.

[1] We present a statistical investigation of dayside magnetospheric erosion based on a survey of 316 cases in 1996–2004. We monitor erosion through the depression in the strength of the terrestrial magnetic field at geostationary heights using magnetic field observations acquired by four GOES spacecraft 2 hours on either side of local magnetic noon. The southward component of the interplanetary magnetic field (IMF) and the solar wind dynamic pressure, quantities which are responsible for opposing effects on the geostationary field, are obtained from the Wind and ACE spacecraft. We extend our previous work to encompass the B_z range [0, −35] nT. We find that dayside erosion saturates when IMF B_z is in the range [−12, −16] nT. This result is consistent with global simulations. With the measured solar wind velocity, this corresponds to an interplanetary electric field (IEF) of 6.2 ± 1.6 mV m^{-1}. We discover that the maximum depression of the geostationary field at saturated erosion is ∼26 nT. In addition, we reveal a direct relation between the saturation of flux erosion of the dayside magnetosphere and that of the cross-polar cap potential (CPCP), both of which occur at approximately the same electric field. For the latter, we apply the Hill-Siscoe model for the calculation of CPCP to our data set. We find the CPCP to deviate from a linear increase with IEF at ∼4 and 7 mV/m, which correspond closely to the IEF range at which we find saturation of dayside erosion to start to manifest itself.

Citation: Mühlbachler, S., C. J. Farrugia, J. Raeder, H. K. Biernat, and R. B. Torbert (2005), A statistical investigation of dayside magnetosphere erosion showing saturation of response, *J. Geophys. Res.*, *110*, A11207, doi:10.1029/2005JA011177.

1. Introduction

[2] The most important mechanism coupling the momentum and energy of the solar wind to the magnetosphere is magnetic field line reconnection between the terrestrial and interplanetary magnetic fields (IMF), particularly when the IMF has a southward component. Continued dayside reconnection opens magnetic flux from the dayside and transfers it to the magnetotail. This process is called ''erosion'' of the dayside because closed flux is being diminished, and consequently, the dayside magnetopause is retreating earthward and the equatorial edge of the polar cap migrating equatorward [*Burch*, 1973]. This removal of open flux proceeds until the field in the tail is strong enough for an instability to develop, leading to the onset of tail reconnection. Tail reconnection closes the opened flux and recirculates it back to the dayside via the flank regions at lower latitudes. In situ observations of erosion were first presented by *Aubry et al.* [1970], who studied magnetopause crossings made by the OGO 5 spacecraft. Studies by *Sibeck* [1994], *Farrugia et al.* [2001], and *Mühlbachler et al.* [2003] deal statistically with erosion as manifested in the geostationary field in the linear stage of flux removal.

[3] Extreme interplanetary conditions, such as very large and negative B_z values, may lead to a nonlinear behavior in the magnetospheric response. Thus for example, the cross-polar cap potential (CPCP) is known to become independent of the interplanetary electric field (IEF), as first suggested on theoretical grounds by *Hill et al.* [1976] [see also *Kan and Lee*, 1979; *Reiff et al.*, 1981; *Hill*, 1984; *Siscoe et al.*, 2002a]. In this case we speak of saturation of response. On the other hand, even under extreme conditions, some properties continue to increase linearly. So does, for example, the ring current enhancement measured by the *Dst* index corrected for dynamic pressure [*Russell et al.*, 2001].

[4] A number of works address the issue of saturation of CPCP. Thus *Russell et al.* [2001] investigated a number of geomagnetic storms and find a linear response of the cross polar cap potential drop to the IEF between 0 and 3 mV/m, with the response becoming nonlinear at higher IEF.

[1]Max-Planck-Institut für Sonnensystemforschung, Katlenburg-Lindau, Germany.
[2]Space Science Center, University of New Hampshire, Durham, New Hampshire, USA.
[3]Space Research Institute, Austrian Academy of Sciences, Graz, Austria.

0148-0227/05/2005JA011177$09.00

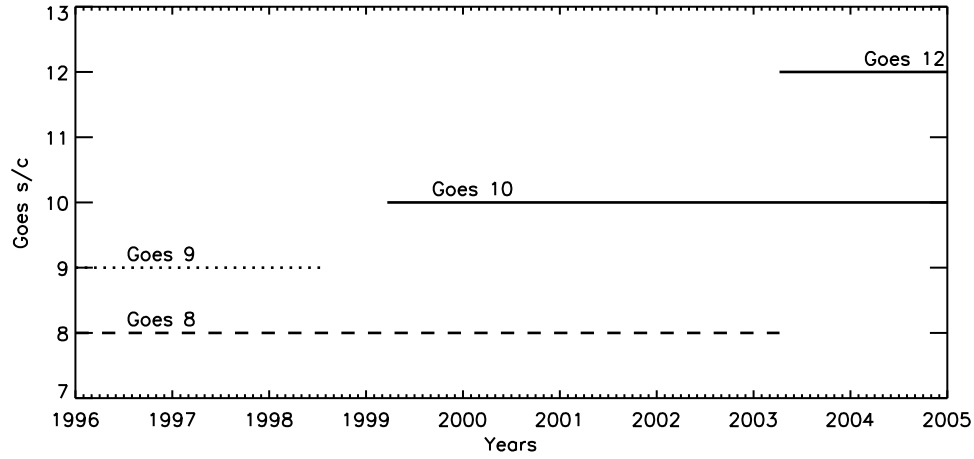

Figure 1. Availability of GOES 8, 9, 10, and 12 spacecraft between 1996 and 2005.

Hairston et al. [2003] established saturation during the strong geomagnetic storm of 31 March 2001, fitting the data to a theoretical model introduced by *Hill et al.* [1976] and formulated definitively by *Siscoe et al.* [2002a].

[5] In the present paper we extend the statistical work of *Mühlbachler et al.* [2003] to large values of southward IMF. We shall show from the behavior of the geostationary magnetic field that erosion indeed saturates, and we shall bracket the B_z range when this happens. Translating this B_z range into an IEF range using IEF = $B_z V_x$, we arrive at practically the same IEF as derived in the references quoted above for the saturation of CPCP.

[6] The layout of the paper is as follows. In section 2 we present the methodology which we applied for this study. First of all we discuss data selection criteria. In the second part of section 2 we describe how we correct the geostationary measurements for the compression produced by the solar wind dynamic pressure. Four individual case event studies are given in section 3.1 arranged in order of increasingly negative B_z. The results over the whole survey are given in section 3.2 and discussed in section 4.

2. Methodology

2.1. Data Selection Criteria

[7] In the following we describe the criteria we have applied to determine the events for this study. As these criteria have already been discussed by *Mühlbachler et al.* [2003], we shall address them here only briefly. All vector quantities are expressed in the Geocentric Solar Magnetospheric (GSM) system.

[8] We obtain the IMF B_z and solar wind P_{dyn} key parameter data for the years 1996–2004 from the Wind and ACE spacecraft via NASA Goddard Space Flight Center's CDAWeb Web site. To ensure that the observed interplanetary characteristics of the plasma and the magnetic field are really responsible for the effects the GOES spacecraft observe, we require further that the interplanetary spacecraft should orbit not far from the Sun-Earth line (y and z of the GSM coordinate system between around -30 and $+30$ R_E, corresponding to a distance perpendicular to the Sun-Earth line of $\sim$42 R_E. This distance is less that the estimated correlation lengths of these two parameters inferred from previous work [see, e.g., *Crooker et al.*, 1982; *Richardson et al.*, 1998; *Matsui et al.*, 2002].

[9] Geostationary magnetic field data are taken from NOAA's GOES spacecraft, which have been providing data from geostationary orbit for more than 2 decades. Figure 1 shows the data coverage of the GOES spacecraft data throughout the years 1996–2004, inclusive, covering most of the current solar cycle to date. GOES 8, marked by the dashed line, was operating from the beginning of our investigations until April 2003. GOES 9 (dotted line) data are available from November 1995 until August 1998, GOES 10 data (solid line) started in April 1999 and continue to the present, and finally GOES 12 data (dot-dashed) replaced GOES 8 since April 2003. To measure the effect of flux erosion at geostationary orbit, we concentrate

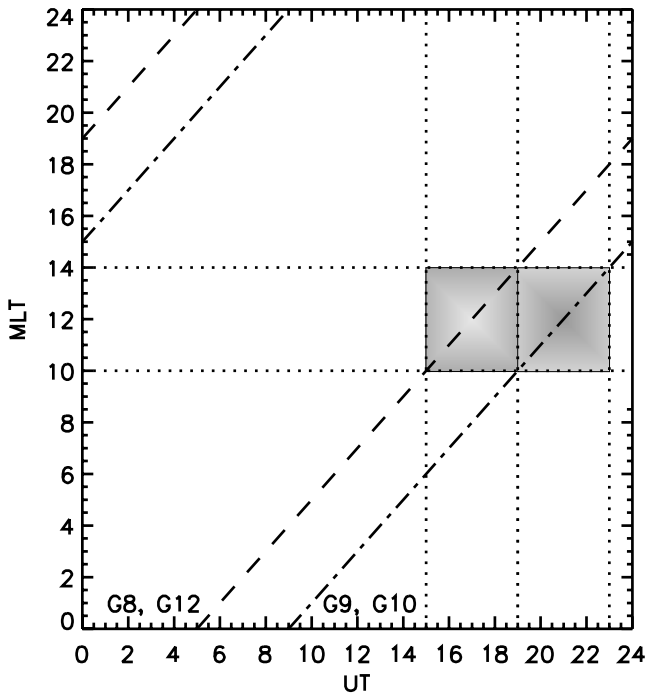

Figure 2. Relation between UT and MLT for GOES 8, 9, 10, and 12 s/c.

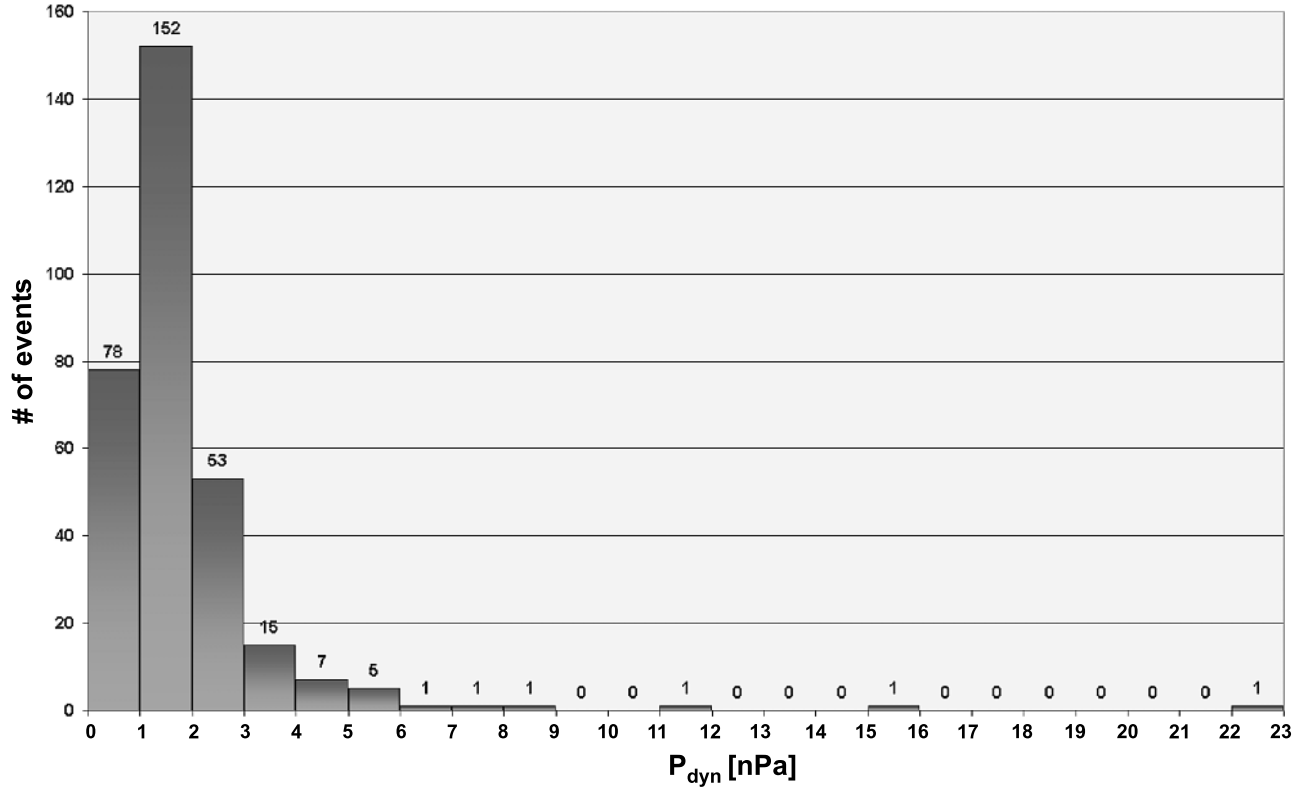

Figure 3. Occurrence of events within steps of 1 nPa of solar wind P_{dyn}.

on time intervals when one of the GOES spacecraft was located between 1000 and 1400 magnetic local time (MLT). Except for a few months between 1998 and 1999, there are always two spacecraft operating at an MLT difference of 4 hours and we thus have a coverage of 8 hours per day of interest for our study. Figure 2 shows the relation between UT and MLT for the GOES spacecraft. Dashed traces show the GOES 8 and 12 positions and dot-dashed traces indicate those of GOES 9 and 10 spacecraft. Dotted horizontal traces indicate 1200 MLT ±2 hours, which in combination with dotted vertical lines mark the UT range of interest (shaded area), i.e., 1500–1900 UT for GOES 8 and 12 and 1900–2300 UT for GOES 9 and 10.

[10] To relate interplanetary B_z and P_{dyn} to the field at geostationary orbit B_{tot}, we take into account the propagation delay time from the solar wind monitor to the Earth's dayside magnetopause. We estimate a convective delay time given by $\Delta t = X/V_x$, with X and V_x being the X-coordinate of the spacecraft and the x-component of the solar wind velocity. In most cases a good timer (e.g., a field and/or flow discontinuity or a distinctive feature in the IMF) could be found to relate the timing of the IMF and GOES field measurements very well.

[11] Further, IMF data are selected if they have more or less constant B_z and P_{dyn} of $\geq$30 min duration. In addition, to compensate for the compression of the magnetic field by P_{dyn}, values of the latter are required to be approximately constant. Finally, we also ensure that as much as possible no other effects influence the geostationary field. Chief among these effects are substorms because they return magnetic flux, stored in the nightside magnetosphere during the growth phase, to the dayside. Thus we try to select data pertaining to the growth phase of a substorm. Substorm onsets may be monitored via the Kyoto *AL* index and identified in magnetograms of auroral zone stations on the nightside. Particularly useful for us are the records of station Tixie from the 210 mm chain (http://stdb2.stelab.nagoya-u.ac.jp/mm210), which is around 0000 MLT when GOES 8 and 12 are near 1200 MLT, and Abisko from the Scandinavian IMAGE magnetometer network for GOES 9 and 10 (http://www.geo.fmi.fi/image/), when the two spacecraft are, in turn, at 1200 MLT.

[12] Applying the above criteria we arrive at a total 316 erosion events. The histograms of Figures 3 and 4 show the distributions of B_z and P_{dyn} in our data set. The distributions are skewed, peaking at $\sim$−5 nT and $\sim$2 nPa, respectively, i.e., fairly typical values at 1 AU. In the case of B_z, most data lie in a range $-12 \leq B_z < 0$ nT. However, there are some events with B_z less than −12 nT, which allow a study of the geostationary field under extreme forcing of the magnetosphere by the solar wind.

[13] Values of the dynamic pressure are mainly below 4 nPa (97.5%). Though the majority of points lies below the long term average of $\sim$2.2 nPa, our survey of P_{dyn} data represents adequately average solar wind behavior and slightly compressed conditions.

2.2. Correction for Dynamic Pressure

[14] For isolating the depression of the geostationary field due to erosion we have to correct the GOES magnetic field measurements for the compression due to the dynamic pressure. *Mühlbachler et al.* [2003] derived the functional form

$$B_{tot}[\mathrm{nT}] = 99.64 + 21.91\sqrt{P_{dyn}} \quad (1)$$

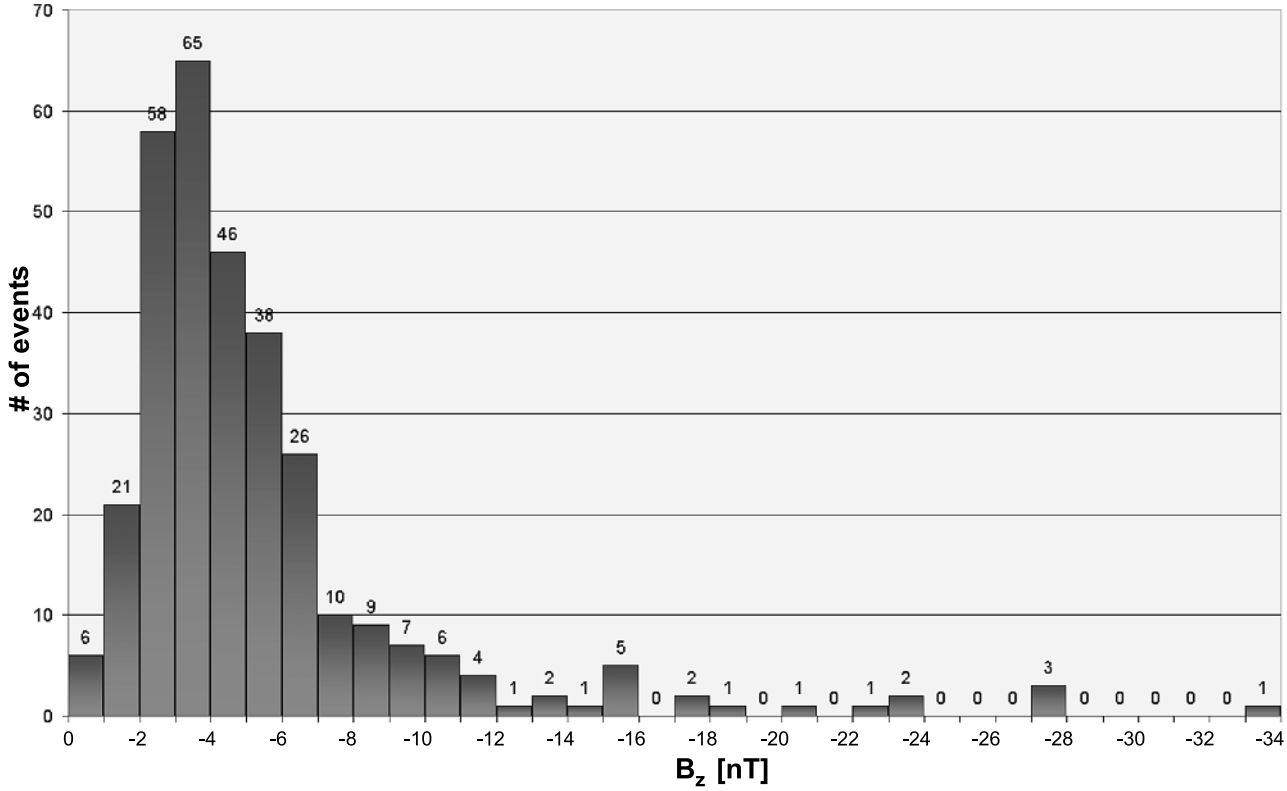

Figure 4. Occurrence of events within steps of −1 nT of IMF B_z.

which was obtained by studying many events characterized by constant P_{dyn} and an IMF clock angle (the polar angle in the GSM *Y-Z* plane) $\Theta < 45°$. This latter condition gives a reasonable guarantee that no dayside reconnection is present [see *Phan et al.*, 1994, 1996]. We shall use (1) here too.

3. Results

3.1. Individual Events

[15] In this subsection we discuss four case studies, data from which are shown in Figures 5–8. The presentation is in order of increasingly negative IMF B_z.

[16] Figure 5 shows data for the time interval 1900–2300 UT on 27 February 1997. The top panel represents the solar wind dynamic pressure as derived from proton velocity and density measurements made by the SWE instrument onboard the Wind spacecraft. The next panel displays IMF B_z measurements from Wind-MFI instrument. Both P_{dyn} and B_z are properly time lagged as discussed. The third panel shows the total field as observed at GOES 9. Local midday corresponds to the time indicated by the vertical dotted line. Finally, panel 4 shows the Kyoto *AL* index.

[17] For our erosion study we concentrate on the interval 2130–2212 UT indicated by a horizontal arrow. During these 42 min, P_{dyn} has an average value of ∼3.48 ± 0.22 nPa, B_z is southward at an average of −13.01 ± 0.43 nT. GOES 9 measures a magnetic field of average strength of ∼126 ± 3.37 nT. We calculate ΔB_{tot} as the difference between the measured B_{tot} and the pressure corrected magnetic field strength as described by equation (1), which results in an erosion-related decrease of −14 nT. The Kyoto *AL* index suggests the presence of two substorms between 2030 and 2230 UT. However, the ground magnetograms of the IMAGE/Svalbard chain, located between 2330 and 0200 MLT, confirm only the substorm at 2100 UT, i.e., that preceding our interval.

[18] We repeat this methodology for each of our events. Table 1 summarizes the measurements and results for the four presented case studies.

[19] As a second case study we present observations of the famous Halloween Storm of 29 October 2003 (Figure 6). Because of a lack of ACE plasma data in the interval of interest, we take density and velocity observations made by the LEP instrument on the geotail spacecraft for calculating the solar wind plasma pressure. We show the period 1500–1900 UT when Geotail was orbiting right in front of the bowshock heading toward dusk. The quicklook data of the Kyoto *AL* index (http://swdcdb.kugi.kyoto-u.ac.jp/aedir/index.html) as well as papers which treat this extreme event indicate the time of onset of a large substorm at ∼1930 UT. *AL* index data have just been available as quicklook jpgs, of which we give a cutout in the bottom panel. Three more substorms may possibly be present at ∼1600 and 1800 UT. Thus following our selection criteria we concentrate on the interval 1826–1854 UT where we are in the growth phase of the huge storm B_z is southward at −23.8 ± 1.5 nT. P_{dyn} is somewhat varying at an average of 3.44 ± 0.51 nPa. The geostationary field in panel three shows a lot of variations whereby the mean trend goes along with the southward rotations of the IMF, in particular the minima shortly before 1700 UT and 1800 UT correlate very well with IMF B_z. The average B_{tot} within the framed

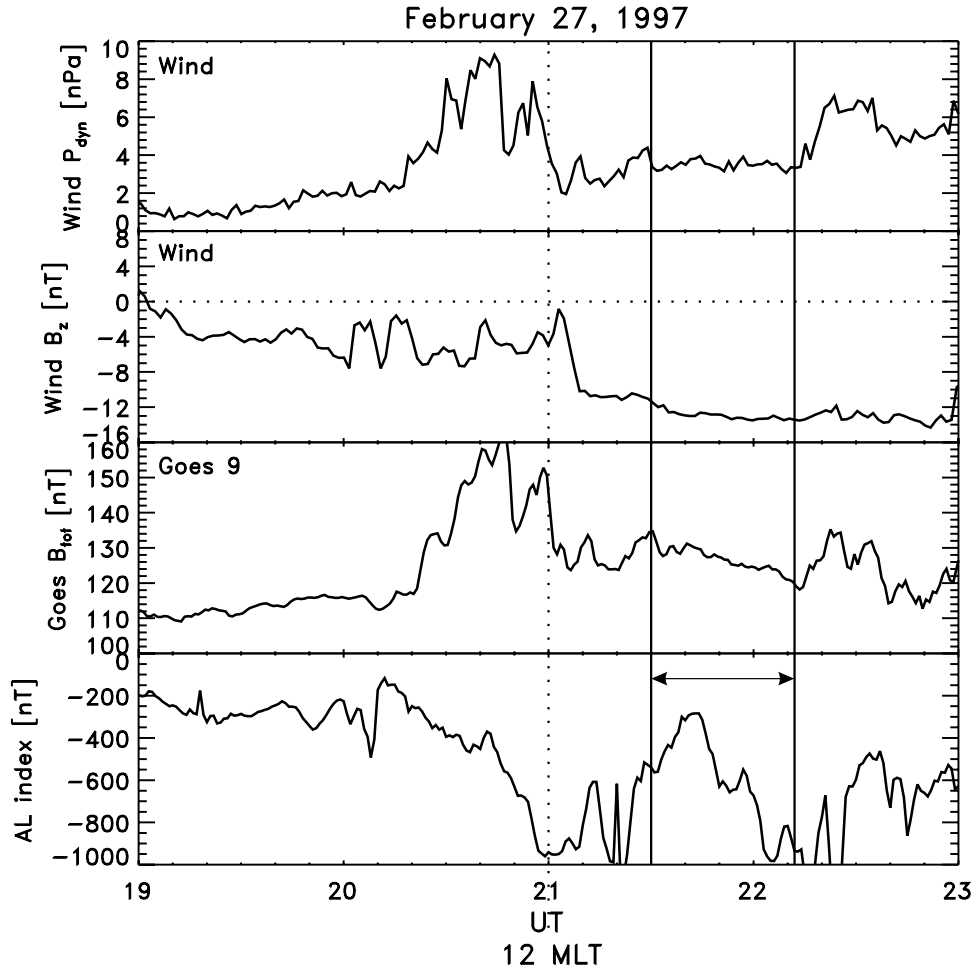

Figure 5. From top to the bottom are the solar wind dynamic pressure from Wind, IMF B_z from Wind, properly time-lagged, the strength of the geostationary field measured by GOES 9, the field depression ΔB_{tot}, and the eight-station *AL* index for 27 February 1997.

interval has strength of 130.1 ± 10.1 nT. Thus the dynamic pressure correction gives geostationary field depression of −10.2 nT.

[20] The most prominent feature in the next case study of 6 April 2000 (Figure 7) is a very disturbed geostationary field after ∼2150 UT. At this time a substorm is monitored at the IMAGE magnetometer chain just as about 1.5 hours before at ∼2115 UT. Thus we suppose to observe an eroded geostationary field during the growth phase of the second substorm between 2109 and 2139 UT at an average strength of B_{tot} = 136.22 ± 4.23 nT. The interplanetary field was at very high negative values during the whole shown interval with an average B_z of −27.81 ± 0.43 nT between the vertical two lines. The observations also show a very strong solar wind dynamic pressure with P_{dyn} = 11.18 ± 0.5300 nPa. After correcting for this, we obtain a geostationary field depression of −36.68 nT.

[21] In Figure 8 (31 March 2001) we show an example of a very extreme event [see also, e.g., *Hairston et al.*, 2003; *Farrugia and Berdichevsky*, 2004] where IMF B_z reached a minimum of ∼ −35 nT. We examine the interval ±15 min around 1600 UT, where at least B_z is rather constant (=−33.64 ± 0.5 nT). Quantity P_{dyn} has a decreasing trend, reflected only partially in the field strength measured at GOES 8, which is fairly constant at an average strength of 119.5 ± 5.6 nT (Table 1). An impressive feature in this data plot is the *AL* index shown in the last panel. A sudden substorm onset can be seen at 1615 UT and thus our chosen interval of interest occurs during the growth phase of a substorm. Correcting for the dynamic pressure we obtain an erosion-related depression of the geostationary field of −18.3 nT.

3.2. Statistical Results

[22] We apply the methodology described in section 2 to the entire set of events to obtain a statistically significant result, which we will then discuss in the next section.

[23] Figure 9 shows the decrease of the geostationary field strength, ΔB_{tot}, as a function of southward IMF B_z, where ΔB_{tot} is calculated as explained above. Stars represent our set of erosion events with vertical lines indicating the error bars in ΔB_{tot}. The linear fit to the data valid for B_z from 0 to −12 nT has the form ΔB_{tot} [nT] = −3.58 + 1.67 B_z. The dashed line shows an extrapolation of this relation to higher values of (negative) B_z. Although measurements for B_z less than −12 nT are, as expected, sparse, it is clear that ΔB_{tot} values lie well below this extrapolation. In particular there is no systematic trend for ΔB_{tot} to decrease for increasingly

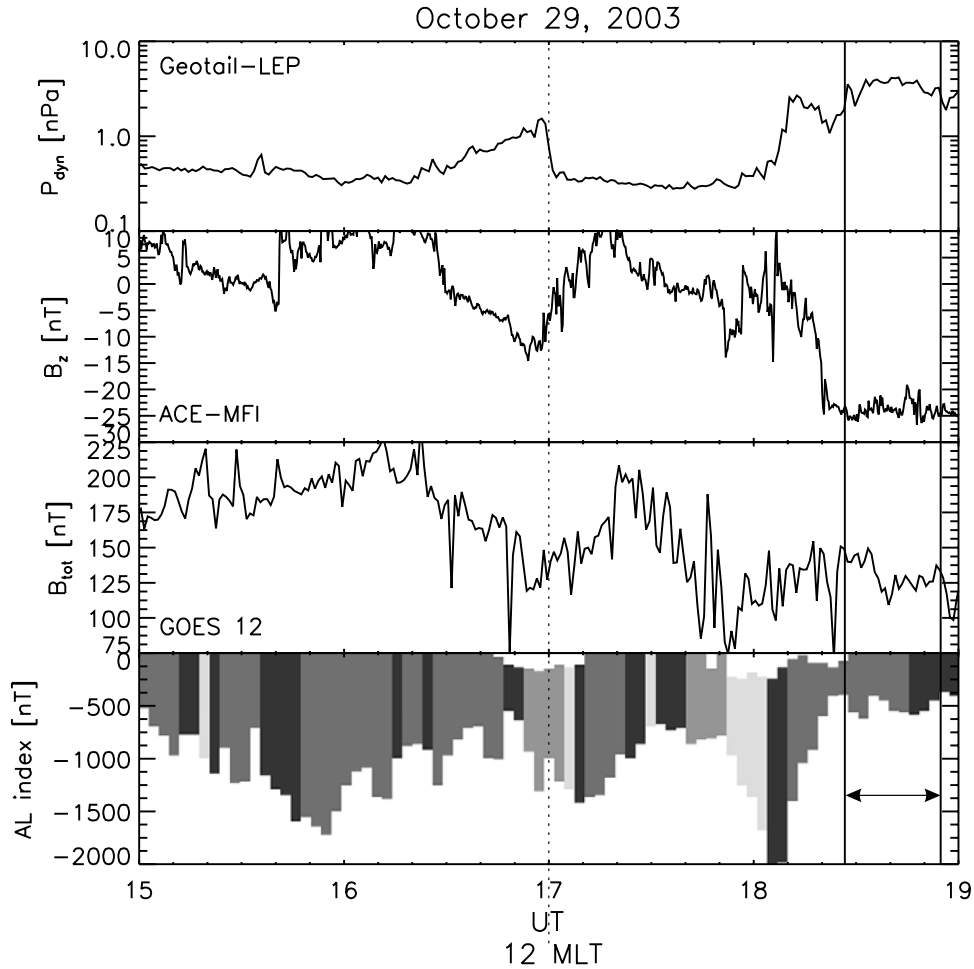

Figure 6. Similar to Figure 5 but for 29 October 2003 with data from Geotail-CPI, ACE-MFI, GOES 12, and quicklook Kyoto *AL* index from their Web site.

negative B_z. This behavior suggests that erosion saturates and Figure 9 suggests further that saturation occurs for an IMF B_z in the range -12 and -16 nT. The associated maximal ΔB_{tot} is on the order of $\sim$26 nT although there is considerable scatter. Taking the eight data points for B_z between -12 and -16 nT, and using the measured solar wind V_x, we find that saturation of erosion sets in at an average IEF of 6.2 ± 1.6 mV m^{-1}. Squares indicate simulations, which are described in detail below.

[24] The spread in the data in Figure 9 and the results of the four case studies clearly show that it is not a straightforward matter to obtain the exact value of decrease in the geostationary field when saturation of erosion sets in. We think that the main sources of errors are (1) a not 100% application of our selection criteria, for example, when a substorm can not be fully ruled out, and (2) when the spacecraft monitoring the solar wind is not exactly inside the ranges we defined in section 2. Nevertheless, we studied each event as carefully as possible, and the quite long list of erosion events allows us to at least perceive a trend.

4. Discussion

4.1. Summary

[25] In the present work we have examined a set of 316 events to investigate erosion of the dayside magnetosphere and to suggest its saturation. The range of B_z examined was $0 \geq B_z \gtrsim -34$ nT. For B_z between 0 and ~ -12 nT the decrease in the geostationary field followed a linear relation with B_z when correction for the dynamic pressure compression was carried out. For more negative B_z the data depart from a linear trend and there is good evidence that the depression of the field at geostationary orbit does not increase further. This occurs when B_z falls in the range -12 to -16 nT. The corresponding interplanetary electric field where saturation of erosion starts to manifest itself is in the range 4.6 to 7.8 mV m^{-1}. It should be borne in mind, however, that interplanetary B_z less than -16 nT are not very common. In addition, we were restricted to 8 hours of local time per day plus having other constraints related to the approximate constancy of interplanetary P_{dyn} and B_z. Thus in a survey ranging over 8 years we found 20 cases with $B_z < -12$ nT and satisfying also these criteria.

4.2. Earthward Retreat of the Magnetopause During Erosion

[26] In an interesting study, *Shue et al.* [2001] studied the standoff distance of the magnetopause r_0 as a function of IMF B_z. The data were for P_{dyn} of 2.2 nPa. They checked three models [*Shue et al.*, 1997; *Kuznetsov and Suvorova*, 1998; *Petrinec and Russell*, 1996]. The first two showed r_0 to approach a limit (model dependent) as B_z goes more

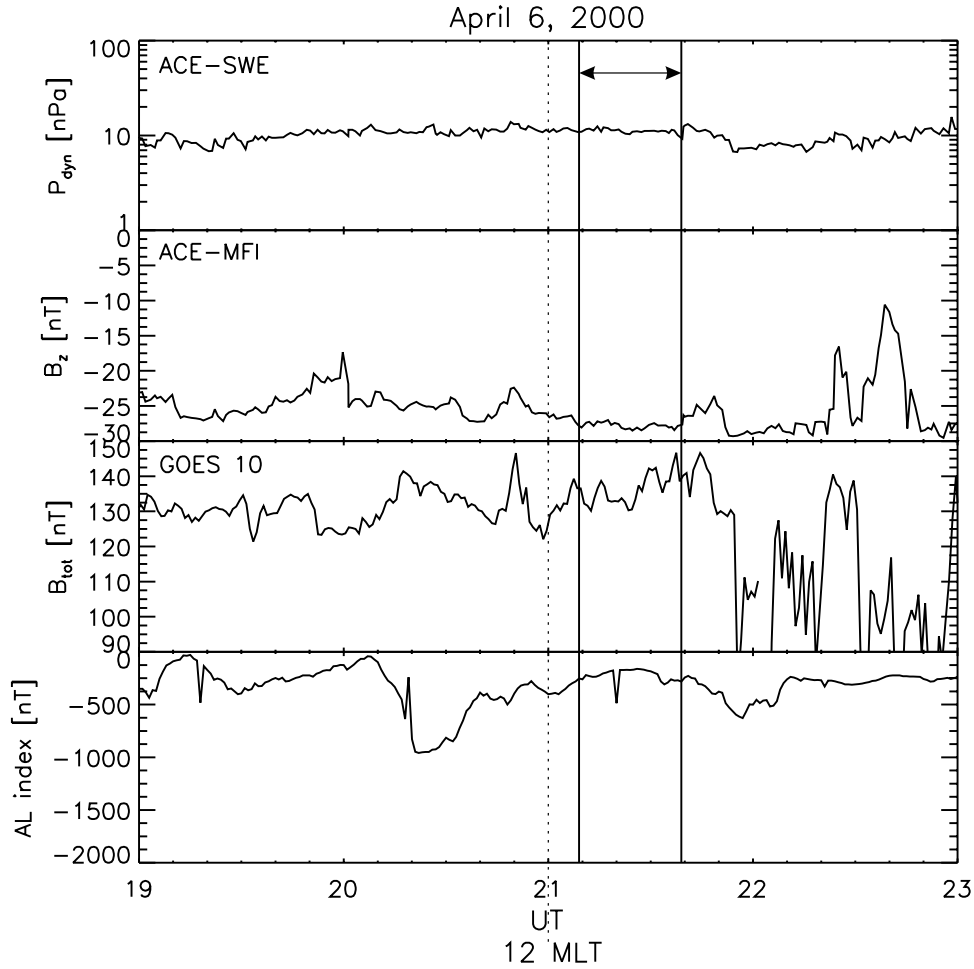

Figure 7. Similar to Figure 5 but for 6 April 2000, with data from ACE-SWE, ACE-MFI, and GOES 10.

negative in the range [−18,10] nT. IMF $B_z < -18$ nT are beyond the scope of Figure 2 in the work of *Shue et al.* [2001]. In the model of *Shue et al.* [1997], r_0 reaches this limit (i.e., ∼8 R_E) at $B_z \approx -15$ nT. Asymptotic limits of r_0 imply that the earthward magnetopause retreat due to dayside erosion has been arrested. Therefore the B_z at which r_0 stops decreasing should correspond to the B_z at which erosion saturates, and indeed this value is roughly what we have obtained from our completely different analysis and approach. This makes the case for saturation of erosion even stronger. Note that P_{dyn} = 2.2 nPa which was used in the *Shue et al.* [2001] study is close to the most common values on our survey (see Figure 3).

4.3. Relation to the Saturation of the Cross Polar Cap Potential

[27] Significantly, our results regarding the value of the IEF when saturation of erosion starts bear close resemblance to those on the saturation of the cross polar cap potential reached by other investigators. Thus in a study of several storm periods for which the IEF reached values as high as 27 mV/m, *Russell et al.* [2001] concluded that the polar cap potential Φ_{pc} stops growing when the IEF exceeds ∼3 mV/m. *Hairston et al.* [2003] studied the storm event on 31 March 2001 and used DMSP measurements of the polar cap potential to compare with the quantitative predictions of a model proposed by *Hill* [1984] and quantitatively calculated by *Siscoe et al.* [2002a] (equation (2) below). They found good agreement with theoretical predictions and concluded that saturation of CPCP can be clearly seen when IEF exceeds ∼8 mV/m. *Siscoe et al.* [2002a] derived the following equation starting from the Hill-Ansatz,

$$\Phi_{pc} = \frac{57.6 E_{SW} P_{dyn}^{1/3} D^{4/3} F(\Theta)}{P_{dyn}^{1/2} D + 0.0125 \zeta \Sigma E_{SW} F(\Theta)}, \tag{2}$$

where E_{SW} is the interplanetary electric field derived via the cross product of the solar wind velocity and the IMF vector, and $F(\Theta)$ is a function of the IMF clock angle, which is taken as $\sin^2(\Theta/2)$ in that study. Parameter D is the Earth's dipole field normalized to 1 for the present value, and Σ is the height-integrated Pedersen conductivity, assumed to be uniform for the sake of simplicity. Finally, ζ is a dimensionless coefficient, for which *Siscoe et al.* [2002a] obtain

$$\zeta = 4.45 - 1.08 \log(\Sigma / 1S). \tag{3}$$

Their baseline case (see their Figure 2) shows a departure from linearity of Φ_{pc}(IEF) at IEF = 6 mV/m. We conclude

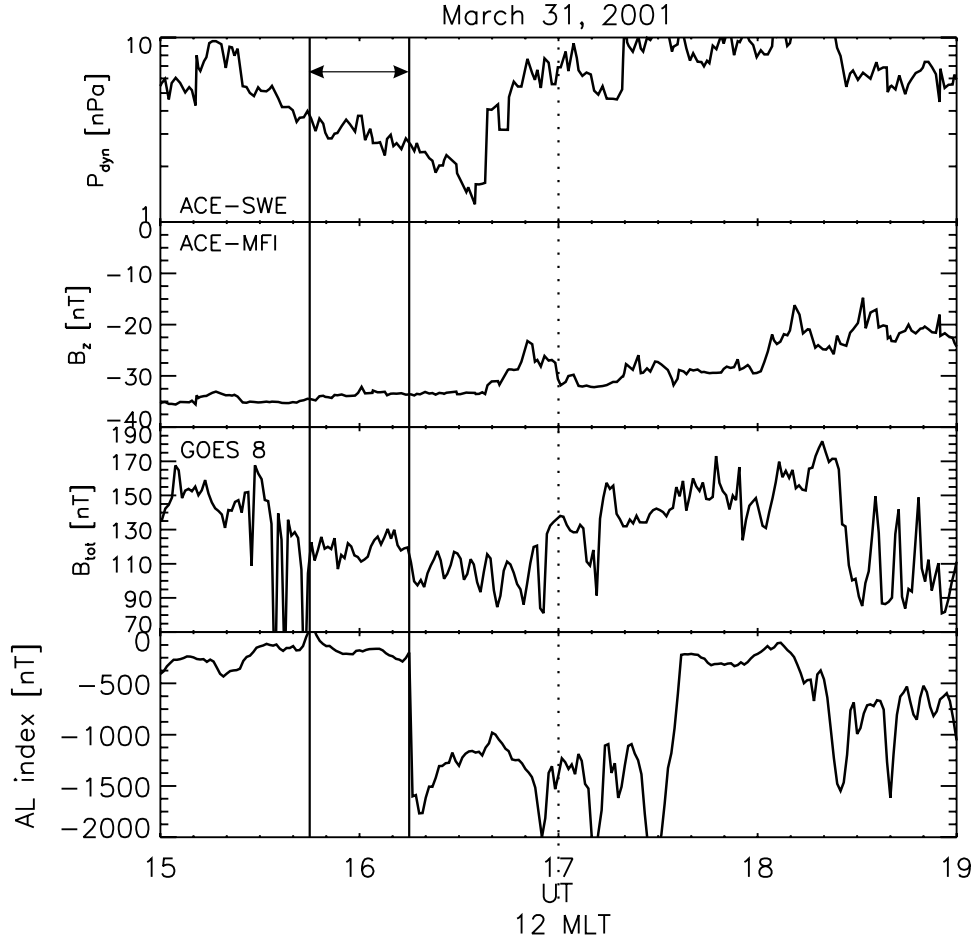

Figure 8. Similar to Figure 6 but for 31 March 2001 and geostationary observations of GOES 8.

therefore that our result for when erosion saturates is in good agreement with these various theoretical and experimental estimates for the saturation of CPCP.

[28] Finally, we would like to see what the Hill-Siscoe formula gives for our data set. For parameters E_{SW}, P_{dyn}, and $F(\Theta)$ we take values averaged over each studied period of our data set. The other parameters are set equal to the same values as in the work of *Hairston et al.* [2003] and parameter Σ is set equal to 10. The results are shown in Figure 10, which presents the calculated Φ_{pc} as a function of the interplanetary electric field. For IEF less or equal to 2.5 the points are fit very well by the straight line $\Phi_{pc} = 12.0 + 26.8\ IEF$ with a correlation coefficient of 0.91 over 217 data points. After $\sim$2.5 mV m^{-1} the calculated points start to depart from a linear trend and to become practically independent of IEF. The highest modeled CPCP is about 300 kV.

[29] Finally, we display Φ_{pc} as derived by the Hill-Siscoe formula by taking $\Theta = 147.8°$ and $P_{dyn} = 1.8$ nPa, which are the average values of the clock angle and the dynamic pressure over all events (dot-dashed line in Figure 10).

[30] In order to further investigate the saturation of magnetopause field erosion, we conducted a number of MHD simulations with parameters similar to the analyzed events. We used the OpenGGCM code [*Raeder*, 2003], which has already been used to investigate polar cap potential saturation [see also *Raeder et al.*, 2001; *Raeder and Lu*, 2005; *Siscoe et al.*, 2004]. The values returned by the code were then corrected for P_{dyn} and plotted with diamond symbols in Figure 9. In the linear regime the MHD results fall within the scatter of the observations. In the nonlinear regime ($B_z > 6$ nT) the MHD results are at the upper end of the observations. There are several reasons for this: (1) the simulations were run without dipole tilt, i.e., at zero magnetic latitude, whereas the observations are from various latitudes ±34 degrees. The erosions is likely strongest at the subsolar point, so observations are likely to show less erosion. (2) Likewise, the observations come from

Table 1. Summary of Case Studies as Presented in Figures 5–8

Date	Period, UT	P_{dyn}, nPa	B_z, nT	B_{tot}, nT	ΔB_{tot}, nT
1997-02-27	2130–2212	3.48 ± 0.22	−13.01 ± 0.43	126.14 ± 3.37	−14.37
2003-10-29	1826–1854	3.44 ± 0.51	−23.8 ± 1.52	130.1 ± 10.1	−10.18
2000-04-06	2109–2139	11.18 ± 0.53	−27.81 ± 0.43	136.22 ± 4.23	−36.6
2001-03-31	1545–1615	3.03 ± 0.4	−33.64 ± 0.53	119.48 ± 5.6	−18.3

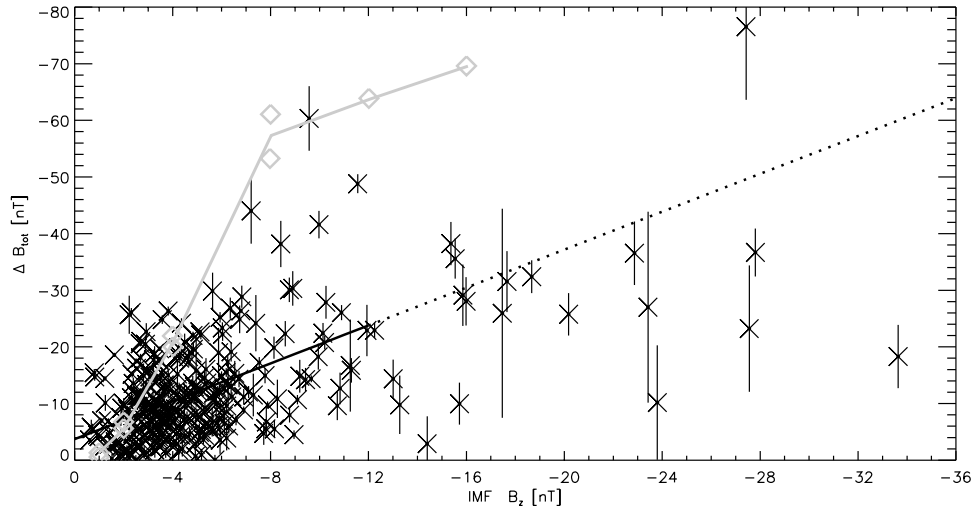

Figure 9. Erosion at geostationary orbit (ΔB_{tot}) as a function of IMF B_z. The solid line shows the linear part of erosion for IMF $B_z > -12$ nT [see also *Mühlbachler et al.*, 2003]. The dashed line extends this line to more extreme $B_z < -12$ nT.

various local times around noon, whereas the simulation results plotted here are exactly from 1200 MLT. Again, the effect is likely strongest near noon, so the simulations represent an upper limit. (3) Most importantly, we found in the simulations that the erosion process takes considerable time. Erosion progresses for 0.5–3.0 hours, depending on parameters, until a steady state is reached. The simulation results shown here are taken after 3 hours of constant IMF conditions when a steady state was reached in all cases. Since the observations represent a random sample of the time elapsed since the southward turning of the IMF, the simulations provide an upper limit here. In fact, it seems that a more thorough investigation of the erosion as a function of southward IMF time, MLT, and latitude/tilt is warranted. We defer this to a subsequent publication.

4.4. Role of the Region 1 Current System

[31] Studies of *Sibeck* [1994] and *Tsyganenko and Sibeck* [1994] concentrate on erosion signatures in the Earth's magnetosphere, e.g., variation of current systems as influencing factors of erosion, decrease of the inner magnetospheric magnetic field. They concluded that the highest contribution to a dayside depression in the terrestrial field comes from the region 1 (R1) Birkeland currents. They expect these currents to produce ~13–26 nT depression

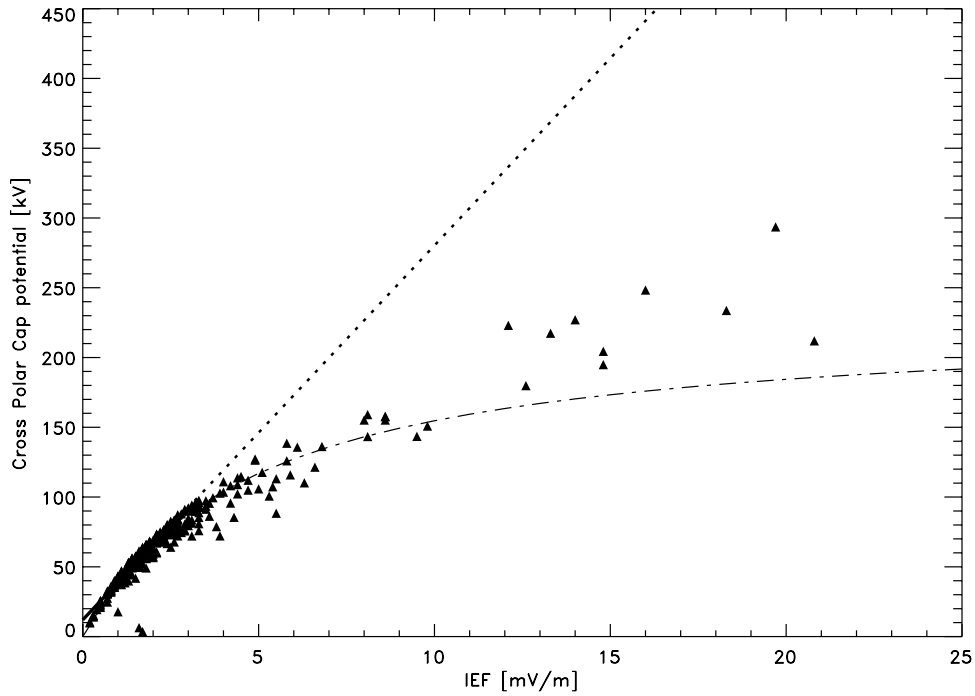

Figure 10. CPCP as function of IEF. The solid line shows a arctan fit.

in the geosynchronous magnetospheric field strength near local noon, lesser depressions within a 6-hour range of local times centered upon noon, and small (<5 nT) magnetic field increases near dawn and dusk flanks. These variations should grow over periods of 20–60 min following southward turning of the IMF. The results in section 3 corroborate their studies quite well. In addition, former theoretical studies of *Hill et al.* [1976] and *Hill* [1984] argue that magnetic fields, which are produced by region 1 currents and which affect the dayside reconnection site, should also reach an upper limit as they tend to cancel with the Earth's dipole field. In their paper *Siscoe et al.* [2002a] calculated these magnetic fields, modeling the R1 current by two circular (Figure 8) current loops in the dawn-dusk terminator plane. They compared the Hill-Siscoe model with MHD simulations and found good agreement. Moreover, *Siscoe et al.* [2002b] studied explicitly the roles of the region 1 current system and the solar wind ram pressure in this context. They concluded that way that when the IEF increases, the region 1 current usurps the Chapman-Ferraro current, which in connection with the dipole field builds the magnetic pressure acting as a counterpart to the ram pressure at the magnetopause. In this way the dayside field is weakened by magnetic fields produced by the region 1 current and the magnetopause has to move earthward until a new pressure equilibrium is reached and no current enhancement is necessary. Thus in contrary to earlier suggestions that the region 1 current is limiting the reconnection rate, the newly reached pressure equilibrium at the magnetopause limits the current that can flow in the region 1 system. We can therefore conclude that there is clear evidence from theoretical predictions as well as our presented observations that (1) the saturation of dayside erosion and the saturation of the cross polar cap potential are related to each other or at least to a common trigger, which (2) most likely is the region 1 current system.

[32] **Acknowledgments.** Part of this work was done while S. M. was working at the Space Research Institute of the Austrian Academy of Sciences and while S. M. was on a research visit to the Space Science Center of the University of New Hampshire. The authors thank K. W. Ogilvie and R. P. Lepping for providing us with key parameter data from the SWE and MFI instruments on Wind, respectively, N. Ness for the key parameter data of the ACE-MFI, D. J. McComas for the ACE-SWEPAM key parameters, H. Singer and D. Wilkinson for the key parameters from GOES spacecraft, A. Viljanen and the German-Finnish-Norwegian-Polish IMAGE project team for Scandinavian magnetometer data (http://www.ava.fmi.fi/image/), K. Yumoto for the preliminary data of the 210 mm magnetometer network (http://stdb2.stelab.nagoya-u.ac.jp/mm210/), and T. Mukai for Geotail-LEP data. We thank the team providing *AL* index at the Kyoto's web page. This work is supported by the Austrian Science Fund under project P17099-N08, NASA WIND grant NAG5-11803, NASA grant on Cluster-Specific Theory and Modeling NASA Living with a Star grants NASW-02035 and NAG5-13512, and NSF grant ATM-0309585.

[33] Lou-Chuang Lee thanks George Siscoe and another reviewer for their assistance in evaluating this paper.

References

Aubry, M. P., C. T. Russell, and M. G. Kivelson (1970), Inward motion of the magnetopause before a substorm, *J. Geophys. Res.*, *75*, 7018.

Burch, J. L. (1973), Magnetic flux erosion, *Radio Sci.*, *8*, 955.

Crooker, N. U., G. L. Siscoe, C. T. Russell, and E. J. Smith (1982), Factors controlling degree of correlation between ISEE 1 and ISEE 3 interplanetary magnetic field measurements, *J. Geophys. Res.*, *87*, 2224.

Farrugia, C. J., and D. B. Berdichevsky (2004), Evolutionary signatures in complex ejecta and their driven shocks, *Ann. Geophys.*, *22*, 3679.

Farrugia, C. J., S. Mühlbachler, H. K. Biernat, and R. B. Torbert (2001), Dayside erosion during intervals of tenuous solar wind, *J. Geophys. Res.*, *106*, 25,517.

Hairston, M. R., T. W. Hill, and R. A. Heelis (2003), Observed Saturation of the ionospheric polar cap potential during the 31 March 2001 storm, *Geophys. Res. Lett.*, *30*(6), 1325, doi:10.1029/2002GL015894.

Hill, T. W. (1984), Magnetic coupling between solar wind and magnetosphere: Regulated by ionospheric conductance?, *Eos Trans. AGU*, *65*(45), 1047.

Hill, T. W., A. J. Dessler, and R. A. Wolf (1976), Mercury and Mars: The role of ionospheric conductivity in the acceleration of magnetospheric particles, *Geophys. Res. Lett.*, *3*, 429.

Kan, J. R., and L. C. Lee (1979), Energy coupling function and solar wind-magnetosphere dynamo, *Geophys. Res. Lett.*, *6*, 577.

Kuznetsov, S. N., and A. V. Suvorova (1998), An empirical model of the magnetopause for broad ranges of solar wind pressure and B_z IMF, in *Polar Cap Boundary Phenomena*, edited by J. Moen et al., p. 51, Springer, New York.

Matsui, H., C. J. Farrugia, and R. B. Torbert (2002), Wind-ACE solar wind correlations, 1999: An approach through spectral analysis, *J. Geophys. Res.*, *107*(A11), 1355, doi:10.1029/2002JA009251.

Mühlbachler, S., C. J. Farrugia, H. K. Biernat, and R. B. Torbert (2003), The geostationary field during dayside erosion events 1996–2001: A joint WIND, ACE and GOES study, *J. Geophys. Res.*, *108*(A12), 1418, doi:10.1029/2003JA009833.

Petrinec, S. M., and C. T. Russell (1996), Near-Earth magnetotail shape and size as determined from the magnetopause flaring angle, *J. Geophys. Res.*, *101*, 137.

Phan, T.-D., G. Paschmann, W. Baumjohann, N. Sckopke, and H. Luehr (1994), The magnetosheath region adjacent to the dayside magnetopause: AMPTE/IRM observations, *J. Geophys. Res.*, *99*, 121.

Phan, T. D., G. Paschmann, and B. U. Ö. Sonnerup (1996), Low-latitude dayside magnetopause and boundary layer for high magnetic shear: 2. Occurrence of magnetic reconnection, *J. Geophys. Res.*, *101*, 7817.

Raeder, J. (2003), Global magnetohydrodynamics: A tutorial, in *Space Plasma Simulation*, edited by J. Buechner et al., Springer, New York.

Raeder, J., and G. Lu (2005), Polar cap potential saturation during large geomagnetic storms, *Adv. Space Res.*, in press.

Raeder, J., Y. L. Wang, T. J. Fuller-Rowell, and H. J. Singer (2001), Global simulation of space weather effects of the Bastille Day storm, *Sol. Phys.*, *204*, 325.

Reiff, P. H., R. W. Spiro, and T. W. Hill (1981), Dependence of polar cap potential on interplanetary parameters, *J. Geophys. Res.*, *86*, 7639.

Richardson, J. D., F. Dashevskiy, and K. I. Paularena (1998), Solar wind plasma correlations between L1 and Earth, *J. Geophys. Res.*, *103*, 14,619.

Russell, C. T., J. G. Luhmann, and G. Lu (2001), Nonlinear response of the polar ionosphere to large values of the interplanetary electric field, *J. Geophys. Res.*, *106*, 18,495.

Shue, J.-H., J. K. Chao, H. C. Fu, C. T. Russell, P. Song, K. K. Khurana, and H. J. Singer (1997), A new functional form to study solar wind control of the magnetopause size and shape, *J. Geophys. Res.*, *102*, 9497.

Shue, J.-H., P. Song, C. T. Russell, M. F. Thomson, and S. M. Petrinec (2001), Dependence of magnetopause erosion on southward interplanetary magnetic field, *J. Geophys. Res.*, *106*, 18,777.

Sibeck, D. G. (1994), Signatures of flux erosion from the dayside magnetosphere, *J. Geophys. Res.*, *99*, 8513.

Siscoe, G. L., G. M. Erickson, B. U. Ö. Sonnerup, N. C. Maynard, J. A. Schoendorf, K. D. Siebert, D. R. Weimer, W. W. White, and G. R. Wilson (2002a), Hill model of transpolar potential saturation: Comparisons with MHD simulations, *J. Geophys. Res.*, *107*(A6), 1075, doi:10.1029/2001JA000109.

Siscoe, G. L., N. U. Crooker, and K. D. Siebert (2002b), Transpolar potential saturation: Roles of region 1 current system and solar wind ram pressure, *J. Geophys. Res.*, *107*(A10), 1321, doi:10.1029/2001JA009176.

Siscoe, G. L., J. Raeder, and A. J. Ridley (2004), Transpolar potential saturation models compared, *J. Geophys. Res.*, *109*, A09203, doi:10.1029/2003JA010318.

Tsyganenko, N. A., and D. G. Sibeck (1994), Concerning flux erosion from the dayside magnetosphere, *J. Geophys. Res.*, *99*, 13,425.

H. K. Biernat, Space Research Institute, Austrian Academy of Sciences, Schmiedlstr. 6, A-8042 Graz, Austria. (helfried.biernat@oeaw.ac.at)

C. J. Farrugia, J. Raeder, and R. B. Torbert, Space Science Center and Department of Physics, University of New Hampshire, Durham, NH 03824, USA. (charlie.farrugia@unh.edu; j.raeder@unh.edu; roy.torbert@unh.edu)

S. Mühlbachler, Max-Planck-Institut für Sonnensystemforschung, Max-Planck-Str. 2, D-37191 Katlenburg-Lindau, Germany. (muehlbachler@mps.mpg.de)